Solitary Fibrous Tumor of the Sinonasal Cavity: CT and MR Imaging Findings

B.T. Yang, Z.L. Song, Y.Z. Wang, J.Y. Dong, and Z.C. Wang

ABSTRACT

SUMMARY: SFT is a rare lesion of the sinonasal cavity. We retrospectively reviewed 5 patients with histopathologically proved sinonasal SFTs to determine their CT and MR imaging features. All patients underwent paranasal sinus CT and MR imaging. Four SFTs occurred in the nasal cavity, and 1, in the maxillary sinus. All SFTs had well-defined margins, and the mean maximum diameter was 55 mm. On nonenhanced CT, 5 SFTs appeared homogeneously isoattenuating to gray matter. The most common manifestations of bony involvement were bony remodeling and thinning. On MR imaging, 5 SFTs were isointense to gray matter on T1-weighted images, and the lesions were isointense in 3 and hypointense in 2 patients on T2-weighted images. The lesions showed heterogeneously marked enhancement on postenhanced MR images. Four patients underwent dynamic contrast-enhanced MR imaging, and the TICs showed a washout pattern. A familiarity with the imaging findings of sinonasal SFT may help to diagnose this entity.

ABBREVIATIONS: Bcl-2 = B-cell lymphoma 2; HU = Hounsfield unit; SFT = solitary fibrous tumor; TIC = time-intensity curve

SFT, first reported in the pleura by Klemperer and Rabin in 1931,[1] is an uncommon spindle cell tumor of mesenchymal origin. This tumor usually arises in the pleura but can also arise in the head and neck, including the sinonasal cavity, orbit, nasopharynx, larynx, parapharyngeal space, oral cavity, and thyroid. SFTs of the sinonasal cavity are rare, with fewer than 30 cases reported in the English literature to date.[2-20] Although several case reports and clinical studies have mentioned imaging findings of SFTs in this region,[6,12,15] the specific imaging characteristics of sinonasal SFT have not been detailed in the literature. We present the CT and MR imaging features of 5 patients with sinonasal SFTs proved by histopathology.

Received July 25, 2012; accepted after revision August 29.

From the Department of Radiology (B.T.Y., Y.Z.W., J.Y.D., Z.C.W.), Beijing Tongren Hospital, Capital Medical University, Beijing, China; and Department of Radiology, Zaozhuang Municipal Hospital, Shandong Province, China (Z.L.S.).

B.T. Yang and Z.L. Song are co-first authors.

Author contributions are the following: study concepts, B.T. Yang, Z.L. Song; study design, B.T. Yang, Z.L. Song; definition of intellectual content, B.T. Yang, Z.L. Song; literature research, Y.Z. Wang, J.Y. Dong; clinical studies, B.T. Yang, Y.Z. Wang; data acquisition, B.T. Yang, Y.Z. Wang; data analysis, B.T. Yang, Y.Z. Wang, J.Y. Dong; manuscript preparation, B.T. Yang, J.Y. Dong; manuscript editing, B.T. Yang, Z.L. Song; manuscript review, B.T. Yang, Z.C. Wang; manuscript revision, B.T. Yang, Z.L. Song, Z.C. Wang.

This work was supported by grants from the Special Fund of Sanitation Elite Reconstruction of Beijing (2011-3-048).

Please address correspondence to Ben Tao Yang, MD, Department of Radiology, Beijing Tongren Hospital, Capital Medical University, No. 1, Dongjiaominxiang, Dongcheng District, Beijing 100730, China; e-mail: cjr.yangbentao@vip

http://dx.doi.org/10.3174/ajnr.A3485

MATERIALS AND METHODS

Patients

This study was approved by the institutional review board. Five patients with histopathologically confirmed sinonasal SFTs diagnosed during an 8-year period (March 2004 to May 2012) were retrospectively reviewed. The female/male ratio was 1:4. The average age was 43.2 years (range, 36–55 years). All 5 patients underwent surgical removal of SFTs by endoscopic sinus surgery. Their clinical presentations, physical and nasal endoscopy examinations, and treatment plans were extracted from the medical records.

CT Technique

All 5 patients underwent paranasal sinus unenhanced CT. Images were obtained in both the axial and coronal planes in all 5 patients by using a LightSpeed 16-section CT scanner (GE Healthcare, Beijing, China) or a Brilliance 64-section CT scanner (Philips Healthcare, Best, the Netherlands). The imaging parameters were as follows: voltage, 120 kV; current, 200 mA; matrix, 512 × 512; and section thickness, 2 mm. These images were reconstructed by using both a bone algorithm (window width of 2000 HU at a window level of 200 HU) and a soft-tissue algorithm (window width of 400 HU at a window level of 40 HU). Reformations were performed from the superior wall of the frontal sinus to the inferior wall of the maxillary sinus in the axial plane and from the anterior wall of the frontal sinus to the posterior wall of the sphenoid sinus in the coronal plane.

MR Imaging Technique

Paranasal sinus MR imaging was performed in all 5 patients before surgery. The MR imaging examinations were performed on a

1.5T unit (Signa TwinSpeed Excite; GE Healthcare, Milwaukee, Wisconsin) or a 3T unit MR imaging system (Signa HDx; GE Healthcare) with an 8-channel head coil. Fast spin-echo pulse sequences were used in these patients. These patients underwent nonenhanced axial and coronal T1WI and axial T2WI and enhanced axial, coronal, and sagittal T1WI. Frequency-selective fat saturation was added in the postcontrast axial or coronal plane. The imaging parameters were as follows: T1WI: TR, 500–600 ms; TE, 10–15 ms; T2WI: TR, 3500–4000 ms; TE, 120–130 ms; excitations, 2–4; echo-train length, 11–27; matrix, 256 × 256; FOV, 18 × 18 cm; section thickness, 4–5 mm; intersection gap, 0.5 mm.

Gadopentetate dimeglumine (Magnevist; Schering, Berlin, Germany) was administered intravenously at a flow rate of 2 mL/s (total dose, 0.1 mmol per kilogram of body weight) by using a power injector (Spectris Solaris; Medrad, Indianola, Pennsylvania) and followed by a 10-mL flush of normal saline solution. Dynamic contrast-enhanced MR imaging was performed in 4 patients by using 3D fast-spoiled gradient recalled imaging before conventional postcontrast T1WI. We used the following scan parameters: TR, 8.4 ms; TE, 4.0 ms; excitation, 1; matrix, 256 × 160; FOV, 18 × 18 cm; section thickness, 3 mm; and intersection gap, 0 mm. Twelve sets of dynamic images were acquired. Each set included 6 images and required 13 seconds; the interset time gap was 12 seconds, and the whole dynamic series took 5 minutes. After the dynamic scan, source images were transferred to an Advantage 4.4 workstation (GE Healthcare) for further analysis. The authors manually drew ROIs on the dynamic images for assessment of the enhancement kinetics of sinonasal SFTs. The area of the ROI was approximately 3–4 mm in diameter. The area that showed the greatest degree of early enhancement was chosen; then, the corresponding TIC could be generated. At the same time, the change in signal intensity of a similar ROI placed on the masticator muscle was used for reference.

Image Analysis

The MR images were interpreted in consensus by 3 authors (B.T.Y., Y.Z.W., and J.Y.D.) with 15, 9, and 7 years of experience in head and neck imaging, respectively.

According to the classification scheme of the dynamic contrast-enhanced MR imaging proposed by Yabuuchi et al[21] and Hisatomi et al,[22] the TICs were analyzed qualitatively as 3 types in the present study: type I (persistent pattern) appears as a straight or curved line, enhancement continues over the entire dynamic study (TTP > 60 seconds); type II (plateau pattern) appears as growing enhancement in the early stage and then displays a sharp bend to form a plateau in the middle and later stages (TTP ≤ 60 seconds; 10% ≤ washout ratio ≤20%); and type III (washout pattern) appears as rapid enhancement during the early stage and then rapidly decreases in the middle and later stages (TTP ≤ 60 seconds; washout ratio > 20%).

RESULTS

Typical clinical manifestations were progressive nasal obstruction (5 patients, 100%), rhinorrhea (4 patients, 80%), intermittent epistaxis (3 patients, 60%), headache (2 patients, 40%), and anosmia (1 patient, 20%). Before diagnosis, the symptom duration of the 5 patients averaged 3.5 years (range, 1.5–8 years). On nasal endoscopy, SFTs appeared as reddish masses with a smooth surface.

Histopathologically, the lesions characteristically displayed plump spindle cells haphazardly intermixed in a attenuated collagenous stroma and prominent vascularity that resulted in a hemangiopericytoma-like pattern. Immunohistochemically, the tumor cells demonstrated positive staining for CD34, vimentin, and Bcl-2.

Four SFTs occurred in the nasal cavity, and 1, in the left maxillary sinus. These lesions were oblong in 4 patients and lobulated in 1 patient and had well-defined margins. The mean maximum diameter was 55 mm (range, 45–64 mm).

On nonenhanced CT, 5 SFTs appeared homogeneously isoattenuating to gray matter. Patchy calcification was identified in 1 patient. All the lesions caused surrounding bony remodeling, thinning, and local resorption (Fig 1*A*).

Five SFTs appeared homogeneously isointense on T1-weighted images relative to gray matter (Figs 1*B* and 2*A*). On T2-weighted images, these lesions showed heterogeneous hypointensity in 2 and isointensity in 3 patients (Figs 1*C* and 2*B*). The lesions typically demonstrated heterogeneously marked enhancement on the enhanced MR images (Figs 1*D* and 2*C*). Multiple tubular flow voids were demonstrated in 2 patients (Fig 1*B–D*). One patient also had intratumoral cystic areas, which showed hypointensity on the T1-weighted imaging and hyperintensity on the T2-weighted imaging, without contrast enhancement (Fig 1*B–D*). Two patients had associated obstructive maxillary sinusitis, and 1 patient had obstructive sphenoid sinusitis, which produced high signal on both the T1- and T2-weighted images, without contrast enhancement (Fig 1*B–D*). One patient's tumor extended into the adjacent nasal cavity and infratemporal and pterygopalatine fossae. Four patients underwent dynamic contrast-enhanced MR imaging, and the TICs revealed a washout pattern (type III), which was similar to that of the internal carotid artery (Fig 1*E*, *-F*).

Five patients were followed up for 0.5–8 years (average, 4.1 years) following endoscopic sinus surgery and showed no evidence of recurrence.

DISCUSSION

On the basis of ultrastructural and immunohistochemical studies, SFTs have been shown to arise from mesenchymal fibroblast-like cells. The definitive diagnosis of the entity depends on the characteristic histopathologic features and specific immunohistochemical markers and patterns of reactivity. Histopathologically, SFTs are characterized by the proliferation of spindle cells arranged in a whorled or patternless fashion within a background collagen stroma and have prominent vascularity in a hemangiopericytoma-like vascular pattern.[2,10,13,15] SFTs show a strongly positive expression for CD34 and moderately positive expression for vimentin and Bcl-2. However, they are usually negative for cytokeratin, antiendomysial antibody, S-100 protein, smooth muscle actin, and desmin; these findings may help to exclude some lesions, like epithelial tumor, hemangiopericytoma, fibrosarcoma, and neurogenic tumor. Immunoreactivity with the marker CD34 was present in all 78 SFTs of the head and neck region reported by Abe et al.[13]

Sinonasal SFTs typically present as a slow-growing painless mass. Previous case series suggest that SFTs in this region show no sex predilection and tend to present after the fourth decade of life,[10,15,17] while our series had a male predominance. Patients generally present with progressive nasal obstruction, rhinorrhea, and epistaxis. Other symptoms, such as anosmia, headache, facial pain, exophthalmos, and visual decrease, may also be present. On nasal endoscopy, SFTs typically appear as a reddish mass with a smooth surface.

According to the literature[5,7,9,11-16,18-20] and the present 5

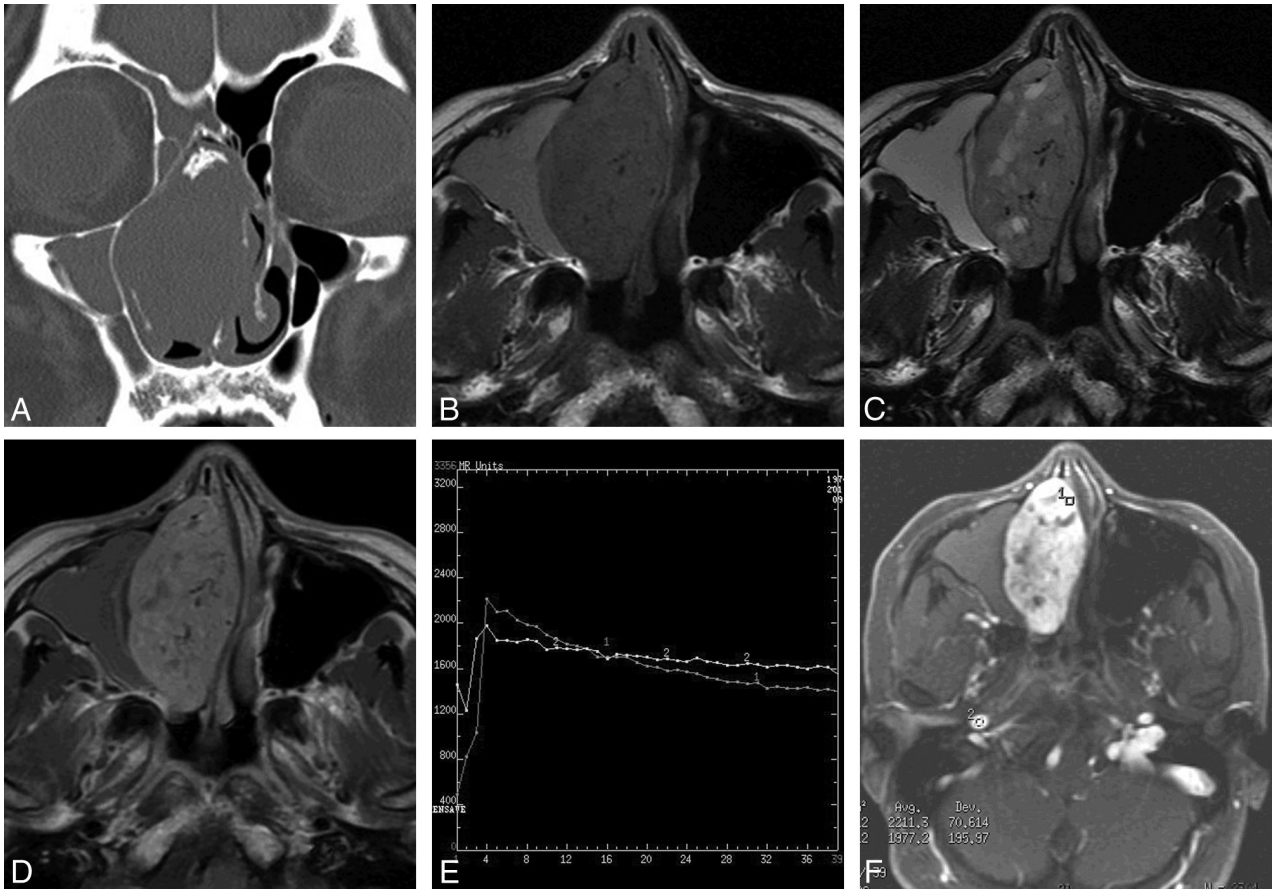

FIG 1. Case 2. *A*, Coronal CT scan with a bone algorithm shows an oblong well-defined mass in the right nasal cavity with patchy calcification. Note remodeling, thinning, and local absorption of the adjacent bony walls. *B*, Axial T1-weighted MR image shows a homogeneous isointense signal mass with multiple flow voids in the right nasal cavity. Note the lesion of high signal intensity in the right maxillary sinus. *C*, Axial T2-weighted MR image shows a heterogeneous isointense signal mass with multiple patchy high-signal-intensity areas, which have no enhancement on the corresponding contrast-enhanced MR images, suggesting cystic degeneration. The lesion in the right maxillary sinus also demonstrates high signal intensity. *D*, Axial contrast-enhanced MR image shows heterogeneously marked tumor enhancement with multiple flow voids. No enhancement of the lesion of the right maxillary sinus is noted, indicating obstructive maxillary sinusitis. *E*, Corresponding axial dynamic contrast-enhanced MR image depicts a washout pattern (type III) TIC. *F*, The round cursors mark the ROIs of the lesion and the right internal carotid artery selected for signal-intensity measurement at dynamic MR imaging.

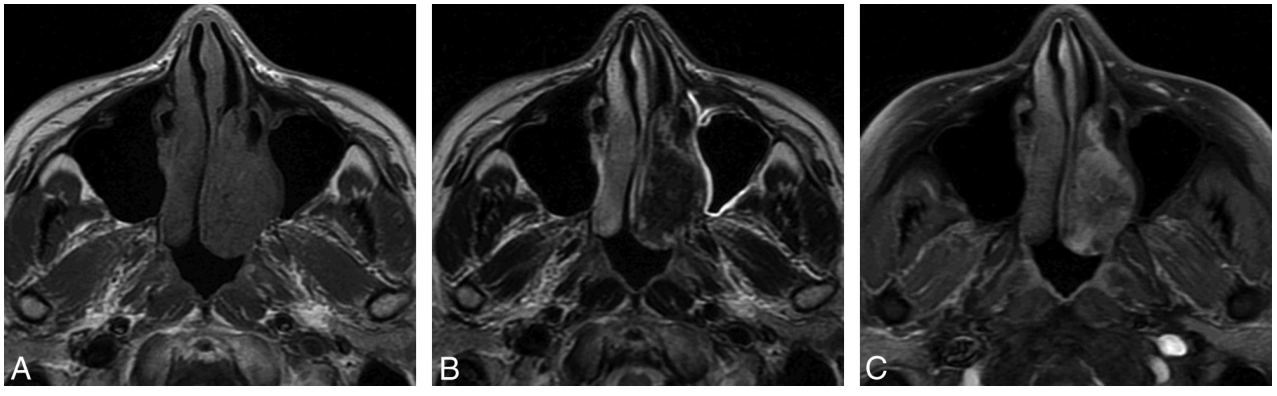

FIG 2. Case 4. *A*, Axial T1-weighted MR image shows an oblong well-defined homogeneous isointense signal mass in the left nasal cavity. *B*, Axial T2-weighted MR image shows a mass with heterogeneous hypointense signal. *C*, Axial contrast-enhanced MR image with fat saturation shows heterogeneous marked tumor enhancement.

cases, most SFTs originated from the nasal cavity and only a minority of cases arose from the paranasal sinuses. Sinonasal SFTs characteristically appear as an oblong well-defined soft-tissue mass. On unenhanced CT, these lesions tend to show homogeneous isoattenuation compared with gray matter, and they usually have marked enhancement after the administration of contrast material. Occasional internal calcifications can be detected, as in case 2 in the present study. Bone remodeling, thinning, local absorption, and even reactive sclerosis can be noted in large sinonasal SFTs. Although this CT pattern is

often seen with sinonasal SFTs, it is nonspecific for soft-tissue tumors of this region.

Compared with CT, MR imaging can demonstrate characteristic features and can be useful in the diagnosis of sinonasal SFTs. These lesions are usually homogeneously isointense to gray matter on T1-weighted images and generally appear heterogeneously isointense or hypointense on T2-weighted images. Predominant low signal on T2-weighted images is unusual for other nasal lesions; this feature is an important diagnostic clue for SFT. Marked enhancement of sinonasal SFTs is generally noted due to their high vascularity, just as 2 of our cases showed multiple flow voids within the tumors, which is also an important MR imaging feature. The typical signal characteristics on T2-weighted images are likely due to fibrous tissue with high collagen content in SFTs.[12,15] Sometimes areas of hyperintense signal within the SFTs on T2-weighted images are identified, which may correlate with hemorrhage, myxoid change, cystic degeneration, or relatively fresh fibrous tissue.[12,15] SFTs typically develop in the sinonasal cavity but may show evidence of local extension into the orbit, pterygopalatine and infratemporal fossa, skull base, or intracranial cavity.[6,11]

Dynamic contrast-enhanced MR imaging may aid in the specific diagnosis of head and neck lesions and predicts their biologic behavior.[21,22] TICs of the 4 patients in the present study showed a washout pattern (type III), which is similar to that of the internal carotid artery. This demonstrates that SFT is a markedly hypervascular lesion and this TIC pattern is unusual for nasal lesions except for juvenile angiofibroma. The TICs of sinonasal SFTs may be related to the hemangiopericytoma-like areas identified histopathologically and to a hypervascular arterial phase blush present on angiography.[23] This technique may give an important clue to diagnose a suspected SFT in the sinonasal cavity.

The main differential diagnosis of sinonasal SFT includes inverted papilloma, hemangioma, juvenile angiofibroma, angiomatous polyps, and hemangiopericytoma. Inverted papilloma typically shows a convoluted cerebriform pattern on both T2-weighted and enhanced T1-weighted MR images. Hemangioma reveals obviously high signal intensity on T2-weighted MR images, with marked enhancement. Juvenile angiofibroma occurs almost exclusively in male adolescent patients. The lesions generally arise in or near the sphenopalatine foramen and thus often are located in the posterior nasal cavity with extension into the nasopharynx. The typical imaging findings include bony remodeling and destruction and marked enhancement associated with multiple flow-void signals on enhanced T1-weighted images. Angiomatous polyps often arise in the choanal region. The lesions usually show hyperintense signal on T2-weighted images and marked enhancement on enhanced T1-weighted images. Hemangiopericytoma is an uncommon tumor in the nasal cavity, which often occurs in the posterior nasal cavity. Bony compression, hyperintense signal on T2-weighted images, and marked enhancement on enhanced T1-weighted images are typical manifestations of hemangiopericytoma.

CONCLUSIONS

Although sinonasal SFT as an uncommon entity, its typical imaging characteristics, including bony remodeling and thinning, isointense or hypointense signal on T2-weighted images, marked enhancement on contrast-enhanced T1-weighted images, and a washout TIC pattern may help to suggest this diagnosis preoperatively.

REFERENCES

1. Klemperer P, Rabin CB. **Primary neoplasms of the pleura: a report of five cases.** *Arch Pathol* 1931;11:385–412
2. Zukerberg LR, Rosenberg AE, Randolph G, et al. **Solitary fibrous tumor of the nasal cavity and paranasal sinuses.** *Am J Surg Pathol* 1991;15:126–30
3. Batsakis JG, Hybels RD, El-Naggar AK. **Solitary fibrous tumor.** *Ann Otol Rhinol Laryngol* 1993;102:74–76
4. Stringfellow HF, Khan IA, Sissons MC. **Solitary fibrous tumour arising in the nasal cavity: report of a case.** *J Laryngol Otol* 1996;110:468–70
5. Kim TA, Brunberg JA, Pearson JP, et al. **Solitary fibrous tumor of paranasal sinuses: CT and MR appearance.** *AJNR Am J Neuroradiol* 1996;17:1767–72
6. Kessler A, Lapinsky J, Berenholz L, et al. **Solitary fibrous tumor of the nasal cavity.** *Otolaryngol Head Neck Surg* 1999;121:826–28
7. Kohmura T, Nakashima T, Hasegawa Y, et al. **Solitary fibrous tumor of the paranasal sinuses.** *Eur Arch Otorhinolaryngol* 1999;256:233–36
8. Konstantinidis I, Triaridis S, Triaridis A, et al. **A rare case of solitary fibrous tumor of the nasal cavity.** *Auris Nasus Larynx* 2003;30:303–05
9. Pasquini E, Cantaroni C, Salfi N, et al. **Endoscopic treatment of an ethmoidal solitary fibrous tumour.** *J Laryngol Otol* 2003;117:889–91
10. Alobid I, Alós L, Blanch JL, et al. **Solitary fibrous tumor of the nasal cavity and paranasal sinuses.** *Acta Otolaryngol* 2003;123:71–74
11. Hicks DL, Moe KS. **Nasal solitary fibrous tumor arising from the anterior cranial fossa.** *Skull Base* 2004;14:203–07
12. Kim HJ, Lee HK, Seo JJ, et al. **MR imaging of solitary fibrous tumors in the head and neck.** *Korean J Radiol* 2005;6:136–42
13. Abe T, Murakami A, Inoue T, et al. **Solitary fibrous tumor arising in the sphenoethmoidal recess: a case report and review of the literature.** *Auris Nasus Larynx* 2005;32:285–89
14. Morales-Cadena M, Zubiaur FM, Alvarez R, et al. **Solitary fibrous tumor of the nasal cavity and paranasal sinuses.** *Otolaryngol Head Neck Surg* 2006;135:980–82
15. Ganly I, Patel SG, Stambuk HE, et al. **Solitary fibrous tumors of the head and neck: a clinicopathologic and radiologic review.** *Arch Otolaryngol Head Neck Surg* 2006;132:517–25
16. Eloy PH, Nollevaux MC, Watelet JB, et al. **Endonasal endoscopic resection of an ethmoidal solitary fibrous tumor.** *Eur Arch Otorhinolaryngol* 2006;263:833–37
17. Furze AD, Peng Y, Myers LL. **Pathology case quiz 2: solitary fibrous tumor of the nasal cavity and ethmoid sinus with intracranial extension.** *Arch Otolaryngol Head Neck Surg* 2008;134:334, 336–37
18. Kodama S, Fujita K, Suzuki M. **Solitary fibrous tumor in the maxillary sinus treated by endoscopic medial maxillectomy.** *Auris Nasus Larynx* 2009;36:100–03
19. Takasaki K, Watanabe T, Hayashi T, et al. **Solitary fibrous tumor arising from the sphenoid sinus.** *Case Report Med* 2009;2009:316042
20. Janjua A, Sklar M, Macmillan C, et al. **Endoscopic resection of solitary fibrous tumors of the nose and paranasal sinuses.** *Skull Base* 2011;21:129–34
21. Yabuuchi H, Fukuya T, Tajima T, et al. **Salivary gland tumors: diagnostic value of gadolinium-enhanced dynamic MR imaging with histopathologic correlation.** *Radiology* 2003;226:345–54
22. Hisatomi M, Asaumi J, Yanagi Y, et al. **Diagnostic value of dynamic contrast-enhanced MRI in the salivary gland tumors.** *Oral Oncol* 2007;43:940–47
23. Dalley RW. **Fibrous histiocytoma and fibrous tissue tumors of the orbit.** *Radiol Clin North Am* 1999;37:185–94